

## Electronic Supplementary Information

For

Description of an original molecular ordering process into a disordered crystalline form : the hybrid displacive – order/disorder character of the low-temperature transformation of linezolid form III

Mehrnaz Khalaji<sup>1,2</sup>, Marta Katarzyna Dudek<sup>1</sup>, Laurent Paccou<sup>2</sup>, Florence Danède<sup>2</sup>, Yannick Guinet<sup>2</sup> and Alain Hédoux<sup>2\*</sup>

Centre of Molecular and Macromolecular Studies of Polish Academy of Sciences,  
Sienkiewicza 112, Lodz, 90-363, Poland

Univ. Lille, CNRS, INRAE, Centrale Lille, UMR 8207 - UMET - Unité Matériaux et Transformations, F-59000 Lille, France

\*corresponding author : [alain.hedoux@univ-lille.fr](mailto:alain.hedoux@univ-lille.fr)

### Contents

- Figure S1: Structural description of Linezolid
- Figure S2: Description of the fitting procedure of the low-frequency Raman spectra collected upon cooling form III
- Figure S3: Description of the fitting procedure of the low-frequency Raman spectra collected upon cooling form II
- Figure S4: Description of the fitting procedure of the mid-frequency spectra (1550 – 1800 cm<sup>-1</sup>) collected at low temperature after cooling forms II and III down to -150 °C
- Figure S5: Description of the fitting procedure of the high-frequency Raman spectra (N – H stretching mode region between 3300 and 3400 cm<sup>-1</sup>)
- Figure S6: Description of the refinements of the X-Ray powder diffraction patterns at 293 K and 373 K.
- Table S1: Results of XRPD pattern refinements at 30 and -160 °C
- Movies

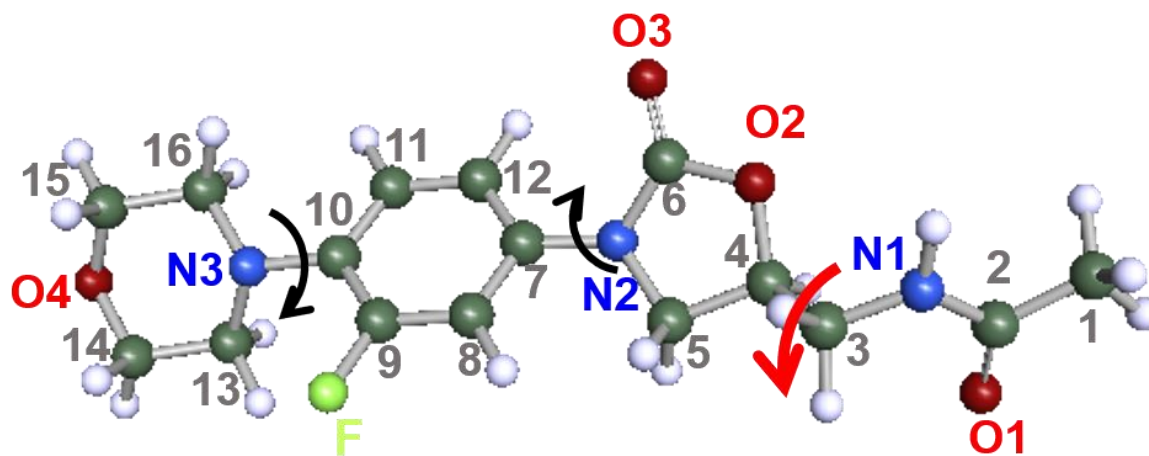


Figure S1. Structural description of linezolid molecule: nitrogen atoms are shown in blue and numbered from 1 to 3, oxygen atoms in red from 1 to 4, carbon atoms in grey from 1 to 16; hydrogen atoms are shown in white and the single fluorine atom is in green. The black arrows correspond to torsion motions considered as different between in the 2 forms (II and III). The red arrow shows torsional motions which should be detected at the very low frequencies from DFT calculations.

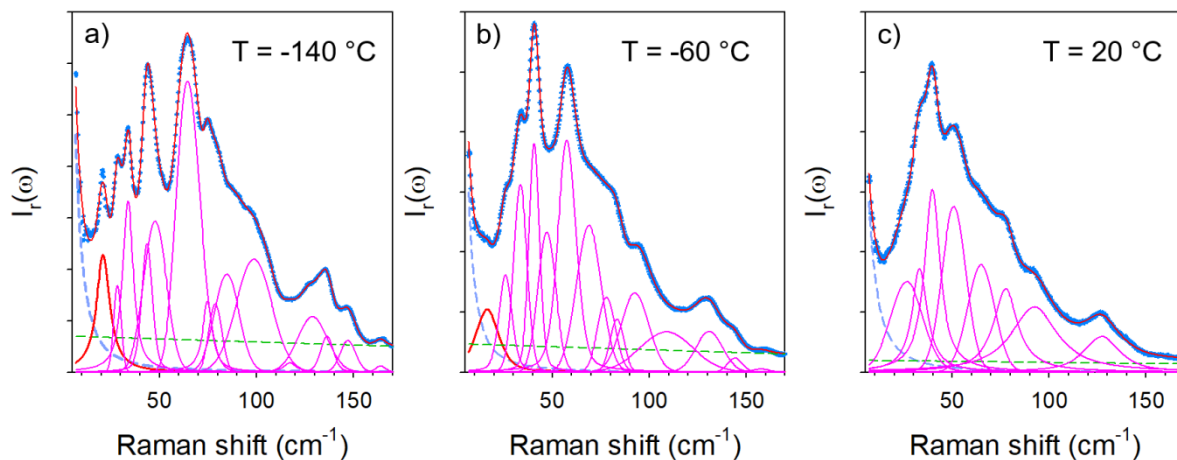


Figure S2. Description of the fitting procedure of the low-frequency Raman spectra collected upon cooling from IV from 20 °C down to -150 °C. The component plotted in red corresponds to the soft mode, not existing at room temperature. The blue dashed-line corresponds to the Rayleigh wing fitted using a Lorentzian function centered at zero. The detection of the Rayleigh wing is inherent to the thermal activation of fast semi-internal motions of atom groups within the molecule which broaden the Rayleigh line, giving rise to the quasielastic intensity.

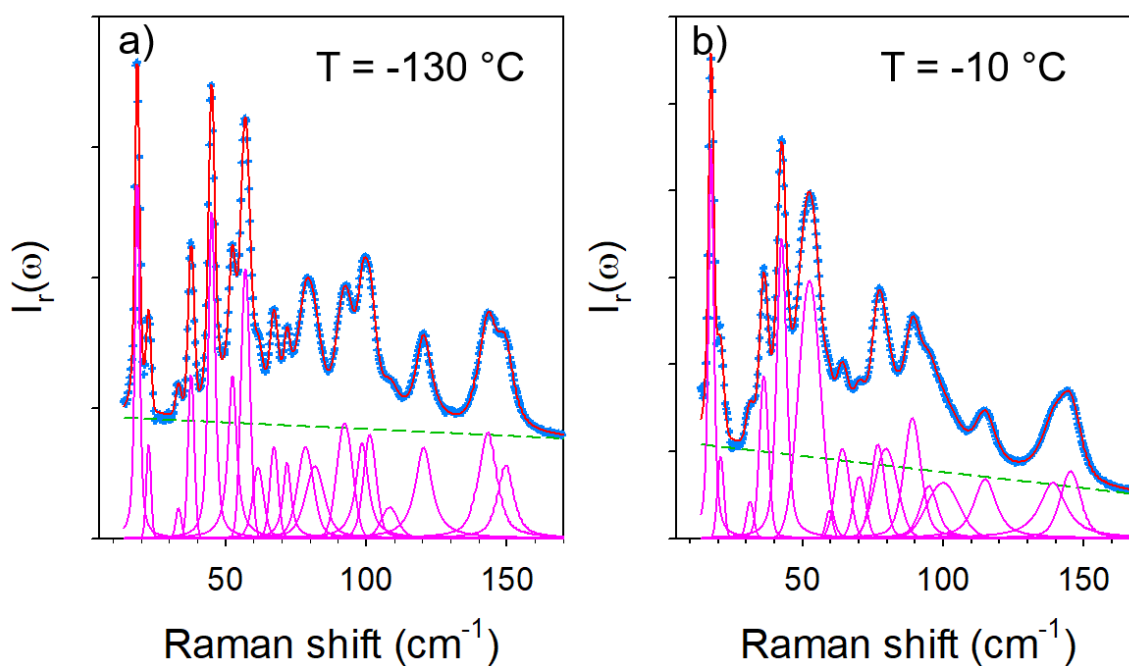


Figure S3. Description of the fitting procedure of the low-frequency Raman spectra collected upon cooling form II from room temperature down to -150 °C. It is worth noting that no quasielastic component was detected in spectra of form II. The main difference between the spectra collected at -10 and -130 °C is resulting from the splitting of the Raman band detected around 50  $\text{cm}^{-1}$  at -10 °C.

T = -150 °C

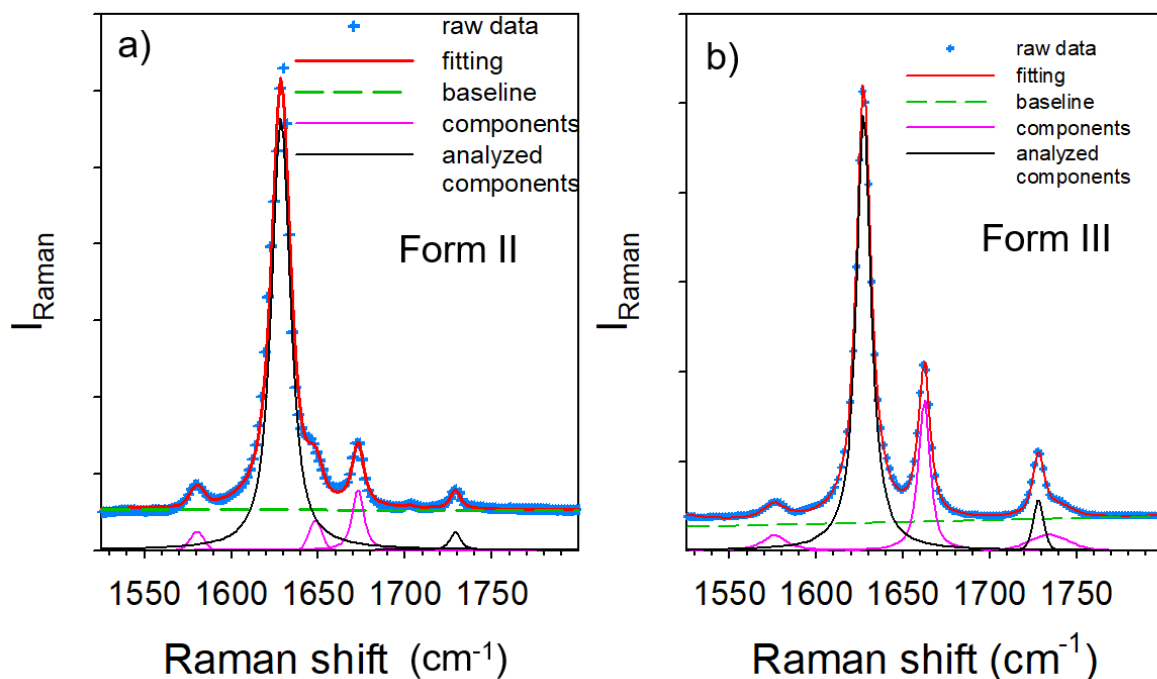


Figure S4. Description of the fitting procedure of the mid-frequency spectra (1550 – 1800 cm<sup>-1</sup>) collected at low temperature after cooling down to -150 °C a) form II and b) form III.

The frequencies of components plotted in black lines were carefully analyzed vs temperature

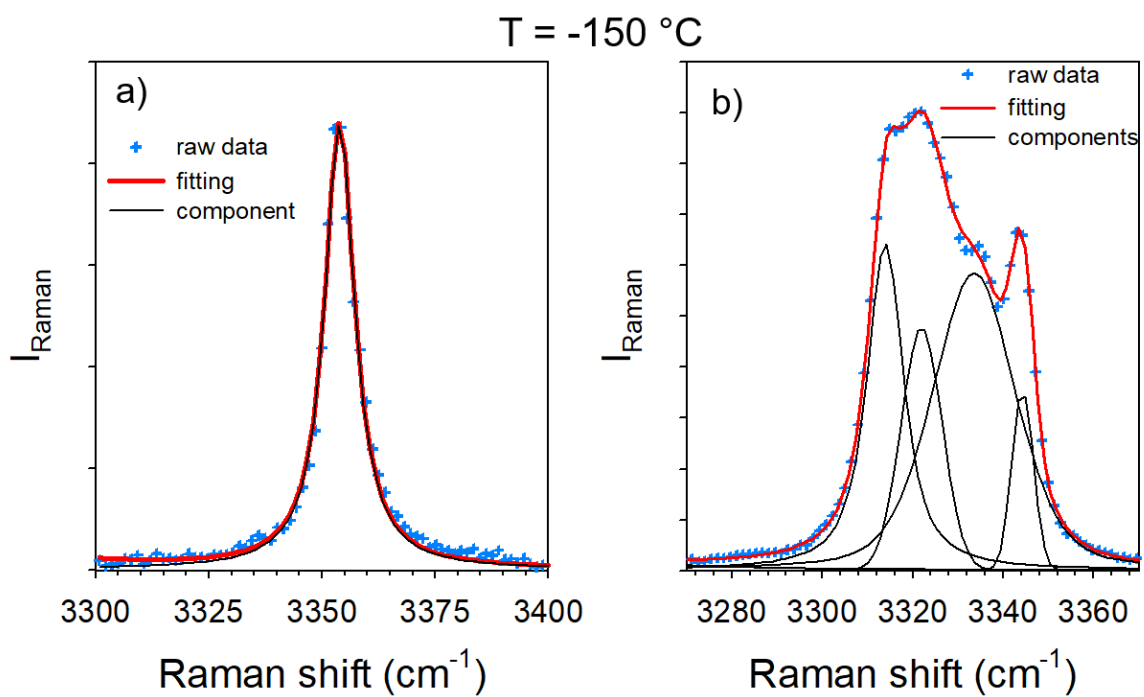


Figure S5. Description of the fitting procedure of the high-frequency Raman spectra (N – H stretching mode region between 3300 and 3400  $\text{cm}^{-1}$ ) collected after lowering the temperature down to -150 °C of a) form II; b) form III

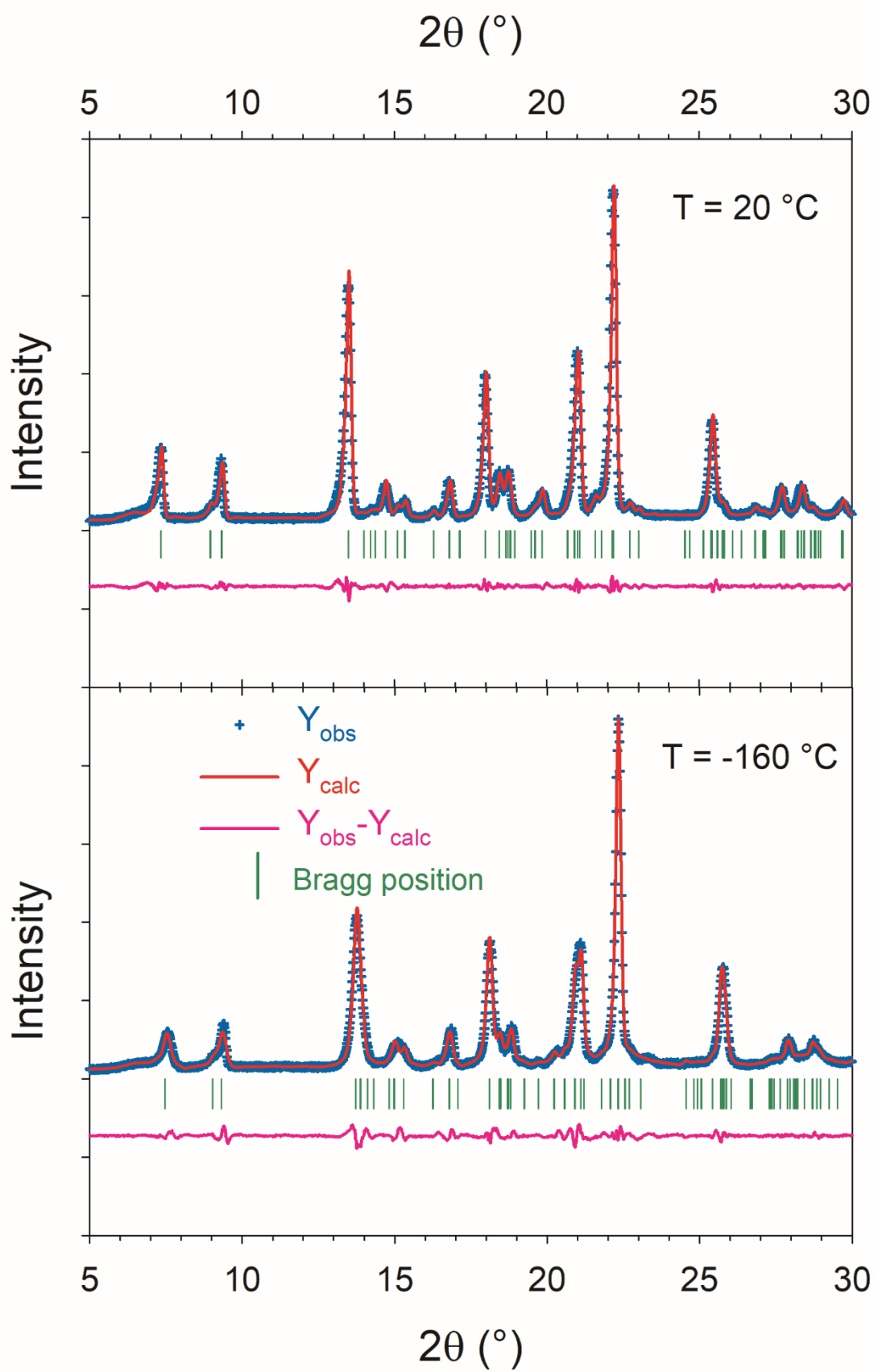


Figure S6: Results of Le Bail refinements at 20 and  $-160\text{ }^{\circ}\text{C}$ .

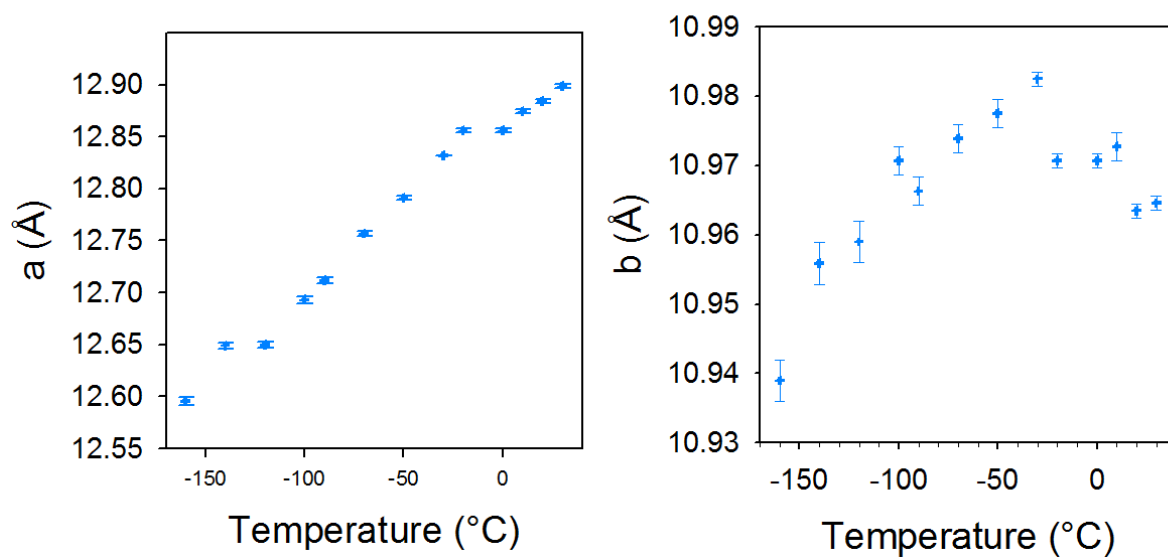


Figure S7: Temperature dependence of a and b parameters obtained from profile matching Refinements.

Crystallographic data obtained after Le Bail refinement	T = 30 °C	T = -160 °C
<p>Crystal data</p> <p>Chemical formula</p> <p>M</p> <p>Crystal system, space group</p> <p>a, b, c (Å)</p> <p><math>\alpha, \beta, \gamma</math> (°)</p> <p>V (Å<sup>3</sup>)</p> <p>Z</p> <p>Radiation type</p> <p>2<math>\theta</math> (°)</p> <p>Data collection</p> <p>Diffractometer</p> <p>Data collection mode</p> <p>Scan mode</p> <p>Step size (° 2<math>\theta</math>)</p> <p>Refinement</p> <p>R factors not corrected from background</p> <p>No of contributing reflections</p> <p>No of fitted parameters</p>	<p>C<sub>16</sub>H<sub>30</sub>FN<sub>3</sub>O<sub>4</sub></p> <p>337.35</p> <p>Triclinic, P-1</p> <p>12.8982(17), 10.9646(12), 6.5778(9)</p> <p>105.7478(66), 88.1916(87), 110.7058(42)</p> <p>835.395</p> <p>2</p> <p>X-Rays, <math>\lambda_1=1.54056</math> Å</p> <p>5 – 30</p> <p>X'Pert Panalytical</p> <p>Bragg-Brentano</p> <p>Linear detector</p> <p>0.0167</p> <p>Rp=0.0338, Rwp=0.0684, Rexp=0.0326</p> <p>66</p> <p>45</p>	<p>C<sub>16</sub>H<sub>30</sub>FN<sub>3</sub>O<sub>4</sub></p> <p>337.35</p> <p>Triclinic, P-1</p> <p>12.5588(35), 10.9277(34), 6.6253(25)</p> <p>106.6047(82), 88.3454(99), 111.2645(61)</p> <p>809.163</p> <p>2</p> <p>X-Rays, <math>\lambda_1=1.54056</math> Å</p> <p>5 – 30</p> <p>X'Pert Panalytical</p> <p>Bragg-Brentano</p> <p>Linear detector</p> <p>0.0167</p> <p>Rp=0.080, Rwp=0.106, Rexp=0.0361</p> <p>66</p> <p>45</p>

Table S1 : Results of XRPD pattern refinements with profile matching option of FullProf program

Movie S1 : internal motions of linezolid giving a contribution to the Raman spectrum around 25  $\text{cm}^{-1}$  from DFT calculations.

Movie S2 : internal motions of linezolid giving a contribution to the Raman spectrum around 35  $\text{cm}^{-1}$  from DFT calculations.

Movie S1 : internal motions of linezolid giving a contribution to the Raman spectrum around 55  $\text{cm}^{-1}$  from DFT calculations.